Design and Characterization of Nozzle Injection Assemblies Integrated with High-frequency Microactuators

John T. Solomon[1], Kyran Caines[2], Chitra R. Nayak[3], Michael Jones[4], and David Alexander[5]

Tuskegee University, Tuskegee, AL, 36088

Two active nozzle injection assemblies integrated with high frequency, resonance enhanced microactuators (REM) have been developed and characterized in this study. In design 1, four injection nozzles each 400 μm diameter were integrated circumferentially to another 1mm nozzle that provides pulsed flow. This actuation jet has a frequency of 13 - 21 kHz. Compressed CO_2 injected through steady nozzles serve as mixing stream, and compressed N_2 generates the actuation jet. The second design flips roles of injection nozzles mentioned in design 1. In this case, actuation jets pulse out through the four nozzles and the steady jet flows through the 1 mm nozzle. In both cases, the REM nozzle flow generates strong compressible vortex in the shear layer of steadily injected fluid that entrain and grow downstream, enhancing microscale mixing of the injected fluid and nitrogen at very high speed, and at a designated frequency. This paper discusses the design and characteristics of REM-nozzles – a potential active injection scheme that can be used for efficient and controlled flow mixing in high-speed applications.

I. Introduction

Efficient and controlled mixing of a fuel with air, moving at very high speed, is a challenging physical problem relevant in supersonic and hypersonic combustion, and it is critical for flight safety and economy [1]. Although mixing is a microscopic, molecular level diffusion problem, the macroscopic phenomena, such as entrainment and

[1] Assistant Professor, Department of Mechanical Engineering, Senior Member AIAA: email: jsolomon@tuskegee.edu, johnts77@gmail.com

[2,4,5] Research Assistants

[3]Assistant Professor, Department of Physics

vorticity dynamics resulting from the shear layer instabilities of the mixing fluids, play a significant role in the overall efficiency of the process. It is well understood that the essential goal of any mixing scheme that involves fluids in motion is to introduce streamwise vorticity in the flowfield [2]. A highly motivating problem is that of air-fuel mixing inside a scramjet engine, a very complex phenomenon involving high-speed interactions of shock and turbulent flow structures within the design constraints of limited residence time and combustor space [3]. Ideally, the injected fuel should mix with the incoming air within a fraction of a second depending on the flow Mach number and the combustor length, for an efficient combustion process and heat release. Due to the short residence time and the compressible conditions existing within the combustor, efficient and controlled mixing remains as an elusive technical challenge. Although significant understanding has been gained on this fundamental problem and researchers have proposed several strategies for efficient fuel injection, robust technologies that can be integrated to the next generation high-speed systems have not been realized yet [4].

For the efficient mixing of air and fuel, researchers have proposed several techniques, passive and active, over the years as indicated in Fig. 1 [5-17]. The passive schemes require no moving parts and tend to be less complicated and less expensive. However, they often do not work well at off-design conditions. The essential goal of these techniques is to generate streamwise, counter-rotational vortices in the flowfield that entrain fuel and air, resulting in increased interfacial area between them for improved diffusion at the molecular level.

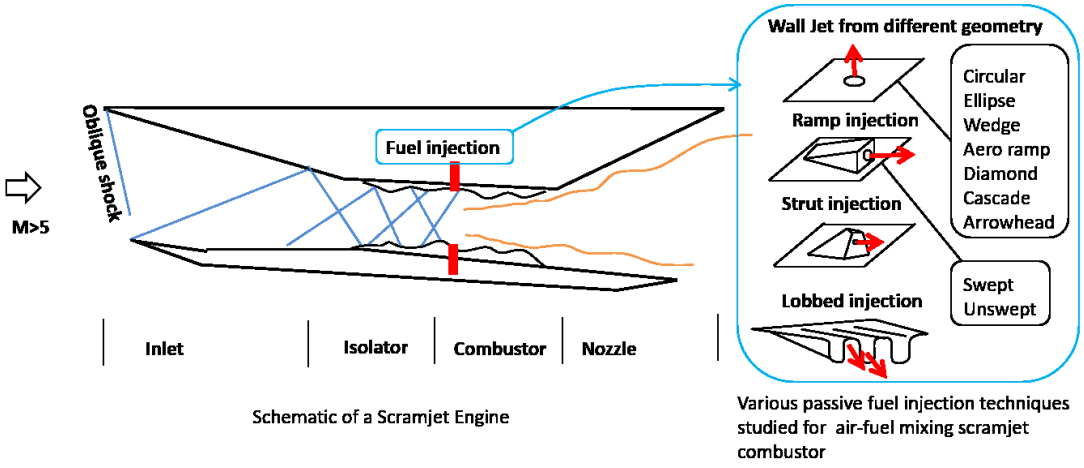

Fig. 1 Current techniques used for improved air-fuel mixing in scramjet engine

Passive flow control has been successfully implemented for improved mixing via geometric modifications using

rigid and fixed fences, spoilers, ramps, and passive bleed system. Passive fuel injection techniques include, but are not limited to, variable-angle injection, circular and non-circular injectors, and small and large vortex/swirl generating tabs and ramps [5-10]. Wall injection at larger angles were observed effective for mixing due to the shock interactions with the free stream that results in enhanced turbulence and increased flow residence time. Forced jets and resulting shock wave-induced schemes were also explored by several researchers for improved mixing in high-speed flows [11, 12]. Passive cavities which are integrated in the combustion chamber have been reported with increased residence time and mixing. The subsonic recirculating flow that forms inside the cavity also serves as a flame holding mechanism in this method [13, 14]. Two classes of parallel fuel injectors that have been heavily studied are the strut and the ramp injectors (Fig. 1). Multi-port fuel placement devices, such as struts protruding into the core flow and large vortex generators such as ramps that induce large axially-rotating vortices, were reported to achieve rapid mixing at higher speeds. The ramps generate large vortices to entrain the air and fuel into one another, thereby increasing the interfacial area of the air- fuel mixing layer. The struts typically generate few vortices and rely on fuel port geometrical modifications to enhance small-scale mixing within the developing air-fuel mixing layer [15].

The active flow control schemes in the form of periodic excitation, on the other hand, require additional system functions as well as some form of energy input. The hypothesis is that introduction of periodic perturbations accelerates and regulates generation of large coherent structures, which are responsible for the jet entrainment through transporting momentum across the shear layers. A typical example of an active flow control scheme is the Hartmann-Sprenger tube, which was reported to have improved mixing with a reduced total pressure loss. In this excited fuel-injection technique, deeper penetration, enriched large-scale structures, and better combustor efficiency were reported [16]. In addition, it is reported that using the correct excited frequency could shorten the mixing and combustion distance, thereby reducing the vehicle size and weight [17, 18]. The current research on fuel injection technologies has been directed towards achieving this goal of deep penetration and rapid mixing of high-speed air and fuel, with less complexity and with a possible handle on its control. Although large bandwidth and deep penetration capability were reported for injection schemes based on plasma phenomena, which are demonstrated to be useful for mixing in supersonic flows, these electro-magnetically driven systems require heavy and complex hardware [19-20]. Additional weight and noise issues could limit integration of plasma-based systems in real life

applications.

Studies show that supersonic pulsed injection is beneficial for scramjets operating over a wide range of conditions. It is reported that the mean penetration was increased using pulsed injection at high frequencies [21]. Also, studies show that pulsed injectors with shorter duty cycle tend to aid the formation of vortex ring structures in the mean flow [22]. While pulsed jets in subsonic crossflow were studied extensively for improved mixing, not many studies have been reported for fuel injectors that operate in supersonic pulsing mode. Used for cross-flow injection, the piston shock tube is an example of an injection system that produces pulsed supersonic flow [23]. The development of an operational and scalable fuel injector that is optimized based on combustion dynamics as well as on overall system performance is essential for the design of next generation scramjet systems with improved safety and fuel economy.

For acoustically modulated jets (using speakers), the penetration and growth rate were reported promising for subsonic cross-flow for a range of modulation frequencies (Strouhal number 0.15-0.35) [37]. But when this approach is applied to supersonic flows, for similar jet velocity and momentum ratio, the pulsing jet requires high stagnation pressure and unsteady amplitude for which such methods becomes ineffective. Moreover, due to the high velocity, the similarity requirement in Strouhal number demands very high frequency. For example, a cross flow sonic jet from a 2mm diameter nozzle needs forcing frequency in the range of ~17-60 kHz (St = fd/U) to keep the Strouhal number (based on exit diameter) range 0.1-0.35, for its natural instability modulation. In this context, powered resonance tubes (PRT) or Hartmann-Sprenger tubes that can operate up to 15 kHz and 150 dB have been demonstrated in supersonic mixing experiments [37]. These studies show that active jet modulation in supersonic crossflow is promising to improve penetration in comparison to unmodulated jets. However, their limited operational bandwidth and large size restrict their implementation in practical systems.

There is a consensus among researchers that the increased penetration of pulsed flow is due to the distinct vortex structures generated. It is believed that frequency of pulsing may have significant impact on mixing, especially when it is close to the natural frequencies present in the flow. There is a need for pulsed injection systems that are capable of penetrating through the high energy boundary layer to induce vorticity into the core of a

combustor flow. We anticipate that the resonance enhanced microactuator system (REM) developed by Solomon et al. is an ideal candidate for such a requirement [24]. In a recent study, the potential capability of REM actuator was proven to induce periodic instabilities in the boundary layer of a supersonic cross-flow [35].

Although the mixing efficiency of a round transverse jet injector can be improved by increasing the jet momentum ratio, this strategy, which results in increased jet penetration and plume size, requires high pressure injection systems and larger cross-sectional area of the engine. The main objective of our study is to develop active fuel injection schemes that can increase local mixing of a fuel in a controlled fashion without much compromise on combustor geometry, jet momentum ratio or penetration depth. Motivated by the subsonic studies that suggest that pulsing cross-flow jets can have better penetration capabilities [21, 22], we explore methods by which a fluid can be injected in a pulsed manner with a bandwidth and momentum suitable for high-speed flow conditions. The first design we propose in this paper is an injector system that uses multiple round injectors integrated around another micronozzle that provides pulsed actuation airflow at very high frequency and amplitude. In the second design, pulsed microactuators were integrated around a 1mm round nozzle to change the natural shear layer instabilities of the jet injected. In a sense, both designs presented in this paper are varieties of round transverse injection, but with a robust, high-frequency, active flow modulation scheme integrated compactly around it.

In this paper, we present the design, development and characterization of two fuel injection assemblies that are integrated with high-frequency, pulsed supersonic actuators that can be operated in a frequency range of 2 – 4 kHz and 13 - 22 kHz. The essential goal is to develop robust active nozzle injection assemblies that can inject a fluid enriched with strong compressible vortices at a designated frequency. To achieve this goal, we considered multiple design options and finally arrived at two, referred to as design 1 and design 2, the details of which are discussed in section III B in this paper. The choice of design I leverages the full potential of REM actuator technology to produce high-frequency pulsed compressible flow [24]. The primary stream CO_2 used in this dual stream design is a non-toxic, cheaper substitute for a fuel. The motivation for this choice is its higher density (1.8 kg/m^3) than compressed nitrogen (1.1 kg/m^3), which is used as the secondary stream for generating the actuation jet. We anticipate that such a choice may also help quantitative microschlieren image analysis of the mixing process. The secondary stream is used for creating/modifying instabilities in the primary stream. In real life situations air can replace nitrogen.

Injecting a fluid (fuel) into the high frequency vortex formation of a secondary stream (oxidizer) may lead to entrainment and possible mixing enhancement at higher velocities. Due to the high velocity of the pulsed vortex, this entrained fuel-air mixture may penetrate deeper into the combustor space further aiding the combustion process. It may be technically feasible to integrate such actuation nozzles close to the injection points wall mounted in a high-speed combustor as indicated in Fig. 1.

While design 1 exploits well-defined instability structures created (compressible vortex) for entrainment, design 2 aims at modification of shear layer instabilities of the injected fluid using pulsed microjet actuators. The motivation for this idea originates from previous flow control studies reported for supersonic impinging jets and free jet noise [32, 36]. The major difference between design 1 and 2 is that one forces the injected stream to follow the vortex entrainment of a high-frequency pulsed actuation jet, the other tailors the natural instabilities of the shear layer of the injected fluid. But in both cases the same REM technology has been used judiciously for its intended purposes. The REM actuator technology used in this study has been developed by Solomon et al. [24-26] can produce pulsed supersonic microjets in a wide range of bandwidth (100 Hz - 60 kHz) and have been proven to be useful for various supersonic flow control applications [27-37]. A brief review of REM actuator technology developed and studied by Solomon et al. [24-26] is provided in section II. In section III, we discuss the design details and experimental set up and in section IV, the results are presented. Section V presents the conclusion and future direction.

II. Resonance Enhanced Microjet (REM) actuators

A schematic diagram of REM actuator is shown in Figure 2*a*. It has three essential components: a primary source jet (under-expanded) which feeds air into a cylindrical cavity, which further expands to a rectangular spreader containing the micro-nozzles.

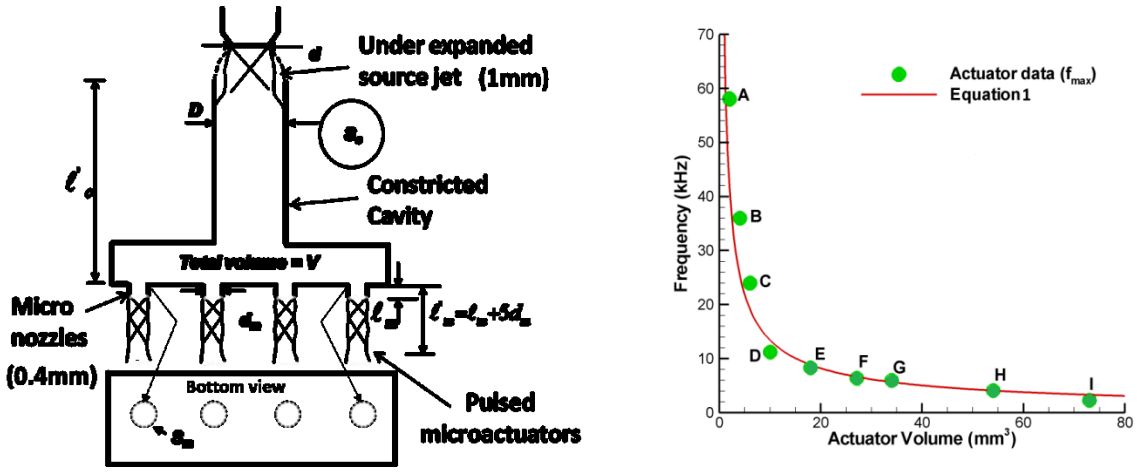

a) b)

Fig. 2 ***a)*** **REM actuator design suggested for practical implementation** ***b)*** **Actuator volume-frequency correlation**

Under certain geometric and flow parametric conditions such as the source jet nozzle pressure ratio, *NPR,* and distance between the source jet nozzle to the cavity entrance, *h*, this actuator configuration can produce pulsed supersonic microjets which will flow through the nozzles at the bottom of the cavity. With extensive parametric studies, Solomon et al. have reported a strong correlation between the actuator's maximum frequencies to its volume, which is summarized in Figure 2*b* [25]. Based on an LEM (lumped element modelling) approach, that considers the actuator as an aero-acoustic resonating system, and with an assumption that acoustic impedance due to the inertance and compliance of the resonating acoustic mass influences its maximum resonance frequency, a semi empirical relation as shown as equation 1 has been suggested as a first-hand design tool for REM actuators [25].

Equation 1 connects the natural resonance frequency response of the actuator system to its geometric parameters as defined in Fig. 2*a*. In this equation the major parameters are the total volume of the actuator *V* and the inflow-outflow cross-sectional area ratio nS_m/S_c, where S_m is the area of each micro nozzles through which pulsed microjets flow and S_c is the area of cross-section of the inflow cavity. Other geometric parameters l'_c *and* l'_m are the effective column length of the fluid resonating inside cavity and outside. If the inflow-outflow area ratio is 1, the

system ceases to resonate [26]. More details of actuator parametric study are available in references [26] and [27]. Note that the frequency-volume relation shown in Fig. 2*b* is derived for actuators that are driven by a source jet from a 1mm exit diameter and therefore the equation (1) is best described for an actuator source jet with mass flow rate equivalent to that used in those experiments. However, for the same geometry and volume of the actuator, it is expected that the use of larger source jet nozzle with increased mass flow rate may lead to higher driving frequencies. This possibility has been explored in the current work for exploiting higher resonating modes of the system.

The capability of an REM actuator to produce pulsed supersonic microjets in the frequency range of 1-60 kHz have been reported by several researchers (Topolski [27], Kreth et al. [28], Puja et al. [29], and Foster et al. [30]). Fluid dynamics of the resonance phenomena and flow physics of the REM actuator were numerically studied by Uzun et al. [31]. Efficacy of this flow control system for suppressing natural instabilities associated with an impinging jet (Strickland et al. [32], Solomon et al. [33]) and a supersonic cavity (Ali et al. [34]) have also been investigated. A recent study has explored REM actuators potential ability to induce instabilities inside the boundary layer of a supersonic M=1.5 cross-flow (35).

III Experimental Details

A. Facility Description

The experiments presented in this paper are conducted in the flow diagnostic laboratory (Fig. 3) recently established at Tuskegee University with support from the US National Science Foundation. The experiments were set up on a vibration free optical table equipped with state-of-the art data acquisition and flow imaging systems. A Photron mini^{TM} high-speed camera is used for image acquisition. This monochromatic camera can capture up to 4000 frames per second at its full resolution of 1024x1024 pixels. A lens based microschlieren system has been set up on the optical table for visualizing the microscale flowfield (Fig. 3). A customized LED light source that can provide pulsed white light having a pulse width of nearly 80 *ns* is used in this microschlieren system. Such a light source with extremely short pulse duration allows us to 'freeze' and capture the high-speed microscale flow structures of the flow domain. In the schlieren system, the light from the LED is focused onto a sharp rectangular

aperture using a condensing lens. This light is then collimated and focused to a point where a sharp knife edge is placed. The actuator flow is kept in the test section for the schlieren imaging. This microschlieren system uses 60 mm diameter lenses with 60 mm focal length for collimating and condensing purposes.

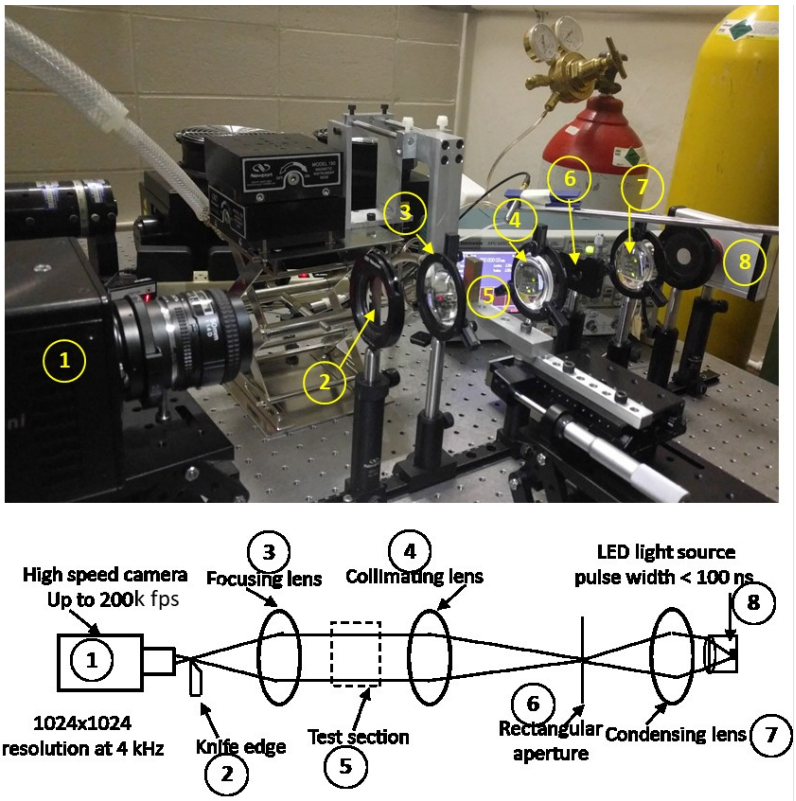

Fig. 3 A schematic of microschlieren imaging set up used for this study

B. Design characteristics of the REM-Nozzles

Figures 4 and 5 shows schematics of the two distinct REM-nozzle assemblies designed and developed for the current experiments. Fig. 4 shows details of the design I that allows pulsed air jet from a 1 mm nozzle at the bottom of the REM block, to interact with the steadily injected fluid (CO_2) from the four 400 micrometer diameter nozzles positioned circumferentially and symmetrically around it. The relative positions of the actuator source jet and the pulsed jet output with respect to the actuator cavity and the steady jet nozzles used for CO_2 injection are also indicated in Fig. 4. The REM actuator integrated to this assembly can produce a pulsed air jet over a frequency range of 13-21 kHz.

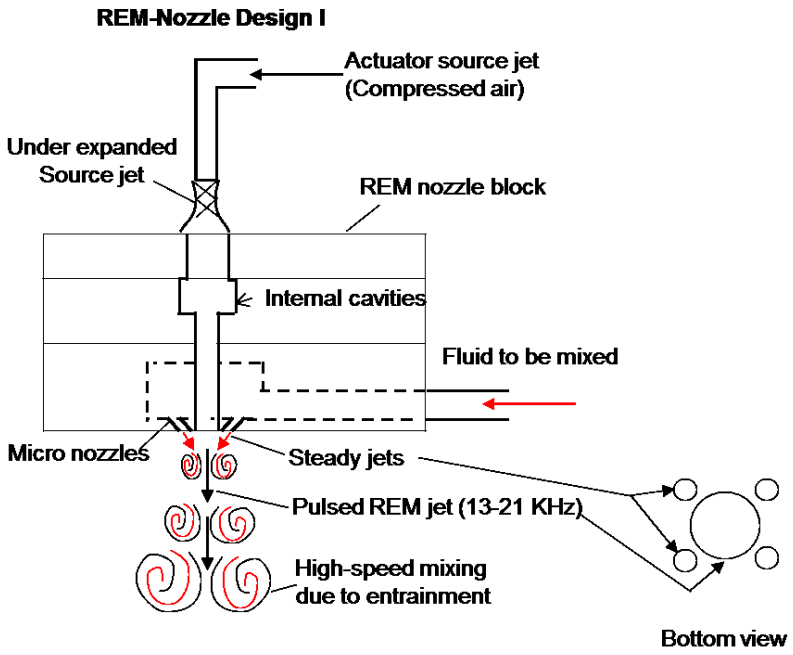

Fig. 4 Schematic of a REM- nozzle assembly Design I

The four micro nozzles, that are inclined 30° to the vertical axis, are used for injecting the mixing fluid into the pulsed air stream. It is anticipated that when the fluid to be mixed (CO_2) is injected into the high-frequency pulsing air jet that flows out through the 1mm central nozzle, strong compressible vortices that are formed due to the pulsing action leads to periodic entrainment of the fluid and air. These vortex structures entrain more fluid, as it propagate downstream with high-speed, enhancing the interfacial area between the shear layers of the pulsed air jet and the CO_2 flow, as indicated in Fig. 4. Evidence of high-frequency evolution of compressible vortex structures and the entrainment phenomena is captured using the microschlieren system. More details of the captured flowfield are discussed later in section IV B.

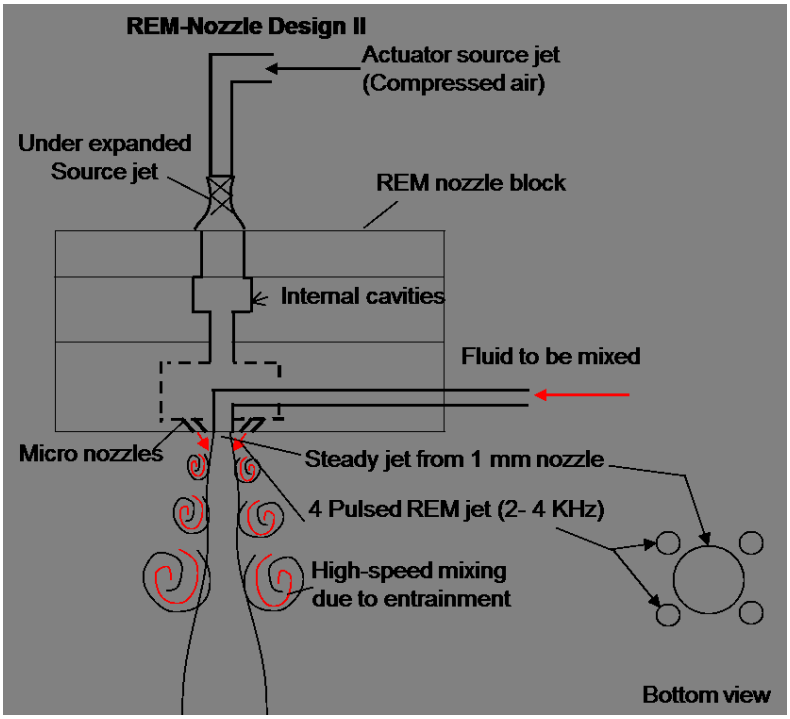

Fig. 5 Schematic of a REM-nozzle assembly Design II

Figure 5 shows the schematic of REM-nozzle design II used in this study. In this case, a steady fluid jet from a 1 mm nozzle at the bottom of the nozzle block is allowed to interact with pulsed microjets from the four 400 micrometer diameter nozzles positioned circumferentially and symmetrically around it. The relative positions of the actuator source jet and the pulsed jets with respect to the actuator cavity and steady jet nozzles used for CO_2 injection are indicated in Fig. 5. The REM actuator integrated to the assembly II can produce pulsed microjets in a frequency range of 2 - 4 kHz. In this case also, the four micronozzles are inclined 30^o to the vertical axis for better entrainment of the mixing fluid with the pulsing jets. In design II, the high frequency pulsing air jets that are injected into the initial shear layer will create microscale vortices in the injected fluid, and it is expected to change its natural instability characteristics in favor of enhanced mixing, as indicated in the schematic shown in Fig. 5.

C. Design details of the REM-Nozzles

Design I: The dimensions of the REM-nozzle design I are shown in Fig. 6. It is fabricated using three brass plates, each of them machined separately with required cavities as indicated in Fig. 6. The top plate has a 3mm long

1.3 mm diameter cavity. The second plate has two cavities. The last plate is integrated with a 1.0 mm ID tube that supplies pressurized CO_2 to a cavity integrated with four 400 micrometer diameter micronozzles. These plates are assembled together without any air leaks. The distance between the central 1mm nozzle and a 0.4 mm nozzle is 0.5mm. This assembly has a total internal cavity volume of 20.6 mm^3 (volume of cavities indicated by red lines in Fig. 6). The under-expanded source jet is supplied from a nozzle of 1.5 mm exit diameter (*d*) and it enters the 1.3 mm cavity on the first plate. This source jet entering the nozzle block produces the pulsed flow through the 1mm diameter tube integrated in the third plate under suitable resonance conditions. This design allows injecting a fluid into the pulsing flow through the four micronozzles in the assembly. The steady CO_2 supply to the chamber while the actuator jet is in operation results in the entrainment of CO_2 into the compressible vortex that is generated by the pulsing jet. The top and bottom views of design I assembly are shown in fig.7. The distance of the exit point of the source jet to the actuator cavity entrance is one of the parameter (*h/d)* that fine tunes the resonance frequency. This parameter is varied from 1.0-1.6 in this experiment. The nozzle pressure ratio *NPR* (ratio of supply pressure to ambient pressure) is another parameter that is used for tuning the pulsing frequency, which is varied from 6.7-8.0 for characterization in the current study.

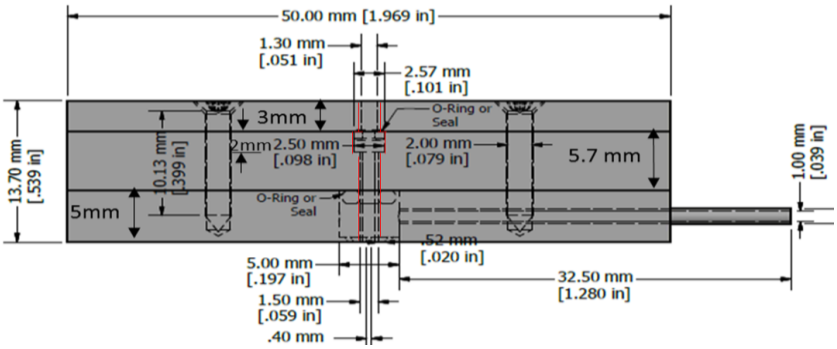

Fig. 6 Design details of REM – nozzle block –I

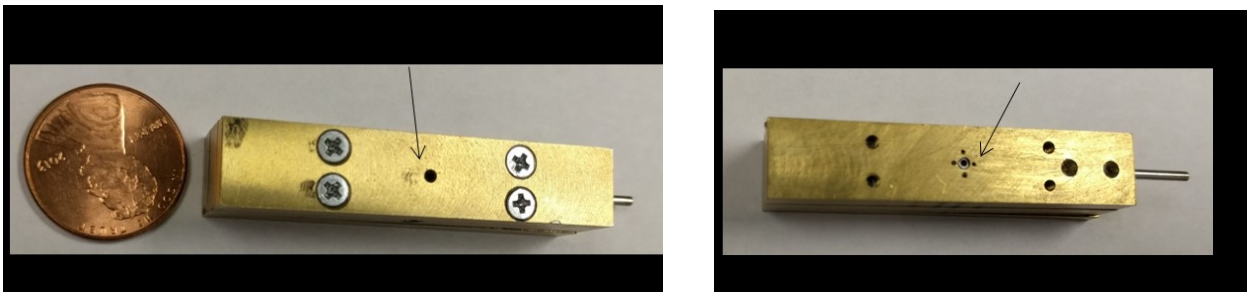

a) ***b)***

Fig. 7 Photograph of REM-Nozzle Block Design I *a*) Top view *b*) The bottom view

Design II: This design uses two brass plates with internal cavities as shown in fig. 8. The top plate has a cylindrical cavity of 1 mm diameter. The second plate has a cavity that is connected to four nozzles as shown in the Fig. 8. The internal cavity has a total volume of 26.7 mm^3 for this design. The source jet is supplied from a nozzle of 1.0 mm exit diameter (*d*) and it enters the cavity on the top plate. The pulsed supersonic jet exits the REM actuator block through four 0.40 mm diameter orifices located at the bottom of the second plate. The nozzle block is integrated with a central 1.0 mm diameter orifice in the bottom plate surrounded by these four orifices. The central orifice is connected to another supply tube separated from the actuator cavity, eliminating mixing of fluid within the nozzle block. A tube of 1.0 mm diameter (ID) supplies CO_2 to this chamber which then steadily flows out through the 1.0 mm central nozzle for mixing experiments. When the under-expanded actuator source jet flows into the actuator cavity at resonating conditions, four pulsed supersonic micro air jet will get injected into the initial shear layers of the central jet. The pulsing actuator interactions lead to modifications in the natural shear layer instabilities of the central jet. The parameter *h/d* is varied from 1.3-1.6 in this experiment. The nozzle pressure ratio *NPR* is varied from 4.5-5.9 for the second design which is found to be the resonating conditions for this design. The photographs of REM-nozzle design II are shown in fig. 9. The **t**op view (Fig. 9*a*) indicates location of actuator cavity where source jet enters the block and the bottom view of nozzle block (Fig.9*b*) shows 4 micro nozzles are surrounded by a 1 mm nozzle through which pulsed jet flows out.

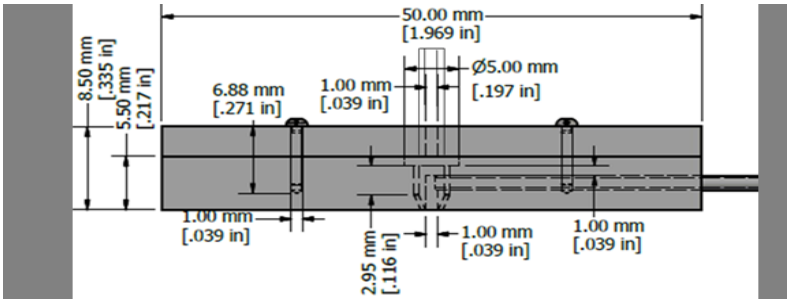

Fig. 8 Details of REM – nozzle block Design II

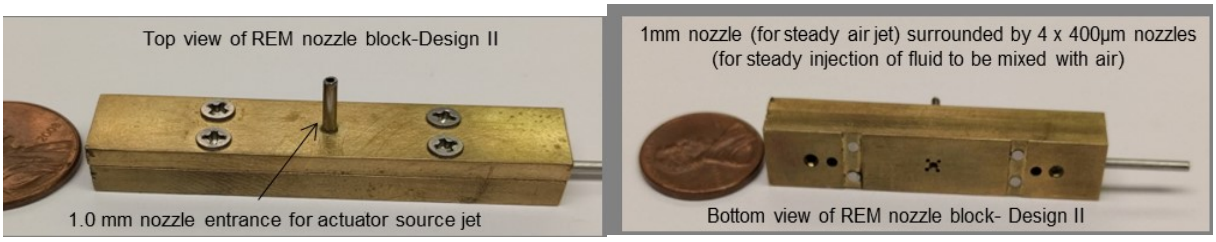

a) ***b)***

Fig. 9 Photograph of REM-Nozzle block II designed for present study *a*) Top view *b*) The bottom view

D. Measurement of nearfield spectra of actuator flowfield

The unsteady spectra of actuator flow field were measured using a GRAS^{TM} 1/4" Free-Field Microphone with a sensitivity of 4mV/Pa located approximately at 45mm (30*d*) and at an angle of 45^{o} from cavity entrance of the REM nozzle block. National Instruments^{TM} 9234, 24-bit, 51.2 kHz data acquisition module is used for acquiring the microphone data using LabVIEW^{TM}. The acoustic spectra was computed using an fft size of 2048 data points. A Hanning window with 50% overlap was used. The source jet pressure is measured with an uncertainty of $\pm$0.1psi. The micro gauge used for linear movements of nozzle block, for varying the parameter *h/d,* has an uncertainty of $\pm$0.01mm.

IV Results and Discussions

A. REM-Nozzle frequency characterization

Figure 10 shows the frequency spectra of the pulsed jet from the REM-nozzle design 1. The microphone used for spectral measurement is located 30 diameters away (45 mm), at an angle of 45^{o} from the cavity as indicated in Fig. 11*a*. When the supply nozzle pressure is varied from *NPR* =6.7 to 8.0, the frequency of pulsing changes from 13.1 to 21.0 kHz. Keeping the *NPR* fixed at 6.7 and varying *h/d* from 1.0 to 1.2, a change in frequency from 18 to 21 kHz is observed (Fig.11*b*). This trend is consistent with our studies reported earlier [26-28] that suggests that *h/d* and *NPR* variation can be used as a fine control knob for frequency tuning in this REM-nozzle block.

The SPL spectra shown in Fig. 10 provide clear evidence to the presence of strong acoustic waves generated by the pulsing supersonic jet in the nearfield. This also substantiates that the REM actuator technology used and integrated to the nozzle assembly can provide high amplitude unsteady actuation to the jets to be injected and mixed. The spectra indicate that the amplitude of maximum frequency response is 50 *dB* above the broadband noise level. The electrical noise level was observed well below 60 *dB* in all measurements. The maximum overall sound pressure level (OASPL) of spectra is measured for *h/d*=1.0 and *NPR*=6.7 as 149.4 *dB* near the source jet when the

microphone is positioned 45 mm away and at 45 degrees from the REM block's upper surface. The frequency of pulsing is 21 kHz in this case.

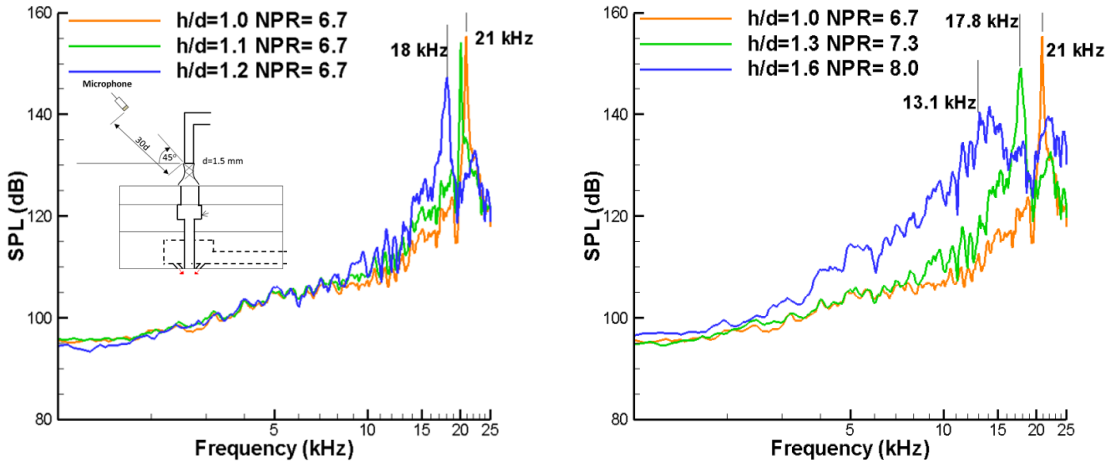

a) **b)**

Fig. 10 Frequency spectra of the pulsed jet measured using the microphone for design 1 with varying a) NPR b) h/d

Fig. 11*a* shows the position of the microphone used for the measurement of nearfield spectra to calculate the OASPL of the REM nozzle flowfield in the source jet side and pulsed flow side. As indicated in Fig.11*b*, the same oscillating frequency of 20.1 kHz is measured at a distance of 140 mm and at an angle of 45° near the source jet and in the pulsing jet side. The OASPL from the measurement at the source side is 134.3 dB and at the exit side is calculated as 121.8 *dB*. The *NPR* and *h/d* are fixed at 6.4 and 1, respectively, in both these measurements. The frequency spectra of actuator source jet and pulsed flow were also measured by microphone positioned at different locations for *h/d*=1 and *NPR*=6.4. At these conditions, the source jet oscillation is measured at 20.1 kHz and the OASPL is measured as 138.7 dB, 134.3 dB and 132.1 dB, respectively, at distances 45, 90 and 140 mm from the actuator cavity entrance. For the bottom side the spectra show same frequency 20.1 kHz and the OASPL is calculated as 126 dB, 122 dB, 118 dB respectively at distances 140mm, 290mm and 420 mm respectively. All these measurements were carried out with a single microphone at different times indicating the repeatability of actuator frequency at the same operating conditions.

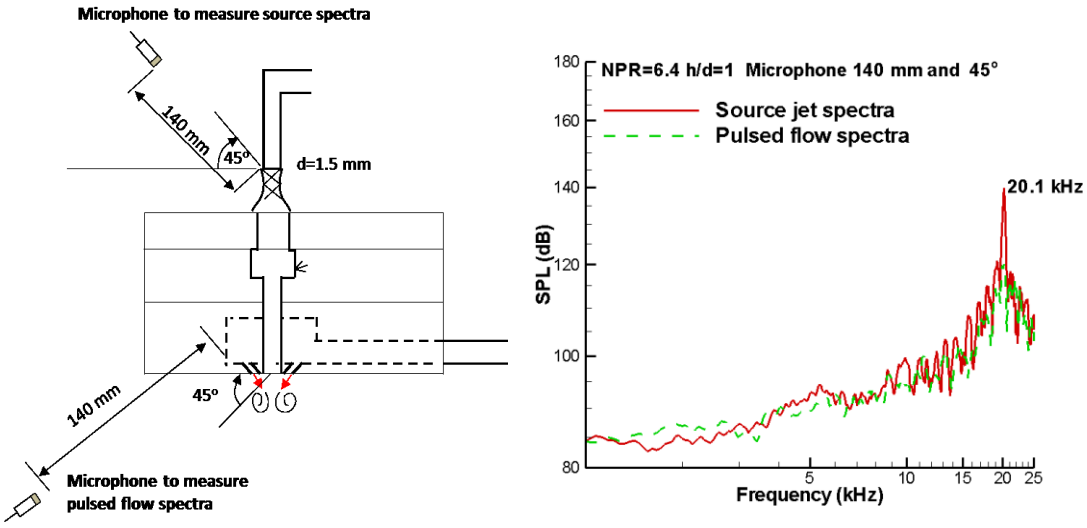

a) **b)**

Fig. 11 Microphone configuration to measure nearfield spectra of REM-Nozzle design I *b)* Frequency Spectra of actuator source jet

Figure 12 shows frequency spectra of the pulsed jet from the REM-nozzle fabricated based on the design II. In this case, a supply pressure variation from *NPR* at 4.5 to 4.7 at constant *h/d* (=1.3) changes the frequency of pulsing from 2.3 to 2.8 kHz. Keeping the *h/d at 1.6,* and varying *NPR* from 5.4 to 5.9, the frequency is tuned from 2.9 to 3.7 kHz. The SPL spectra of the actuator assemblies confirm that strong acoustic waves are generated by the pulsing supersonic jet in the REM nozzle nearfield. This data provides confirmation that the REM actuator technology integrated to the nozzle assemblies can provide high amplitude unsteady actuation to the jets to be injected and to be mixed at high speed.

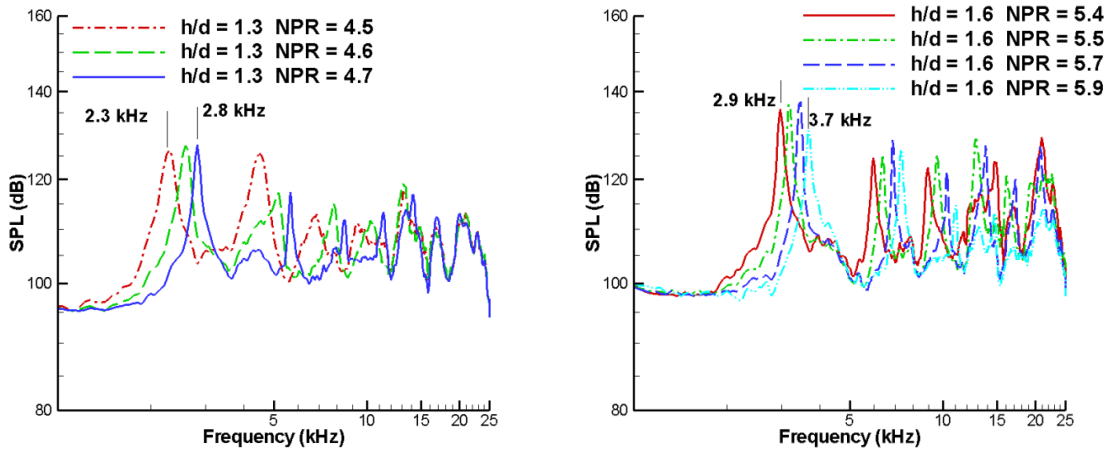

a) b)

Fig. 12 Frequency spectra of the pulsed jet measured using the microphone for design II

The REM-nozzle frequency spectra shown in Figure 12 indicate that the amplitude of the maximum frequency response is more than 30 dB above the broadband noise level for design II, in comparison to the design I where it was measured 50 dB above the broadband noise. This difference is attributed to the fact that design I uses a source jet from a 1.5 mm nozzle, while design II uses it from a 1 mm nozzle. It is reasonable that unsteady oscillations of a larger actuator source jet create higher amplitude pressure oscillations in the nearfield. The electrical noise level was observed well below 60 *dB* in all measurements. For the design II, the maximum OASPL is measured as 139 *dB* for *h/d*=1.6 and *NPR*=5.7 where the frequency of pulsing is measured as 3.6 kHz.

B. Comparison between the previous design correlations and the current designs

Figure 15 shows a comparison of the current data to the correlation (Equation 1) suggested for REM actuator design that connects the maximum resonance frequency of actuator and its volume, essentially a re-plot of Fig. 1*b* with new data points from this study. Note that actuator data summarized in fig 15 was measured for an actuator source jet from a nozzle of 1 mm diameter [25]. However, designing actuators operating in ultrasonic (20 kHz or above) will require a smaller actuator volume (5-6 mm^3) which will be a constraint from a fabrication point of view. The design volume of the REM nozzle is 20.5 mm^3 which predicts a frequency of 8.1 kHz if used with a source jet

diameter of 1 mm. For design I we used a source jet nozzle of diameter 1.55mm (±0.05mm) that provides 2.4 times more mass flow than a 1mm nozzle. Since the mass flow rate to the actuator decides the filling and discharge phase, we anticipated a linear correlation between mass flow rate and resonance frequency. In this configuration, we expected a frequency which will be 2.4 times of 8.1 kHz, which is approximately equal to 20 kHz. The data shows that REM-nozzle block based on design I has maximum frequency around 21 kHz which is close to this prediction.

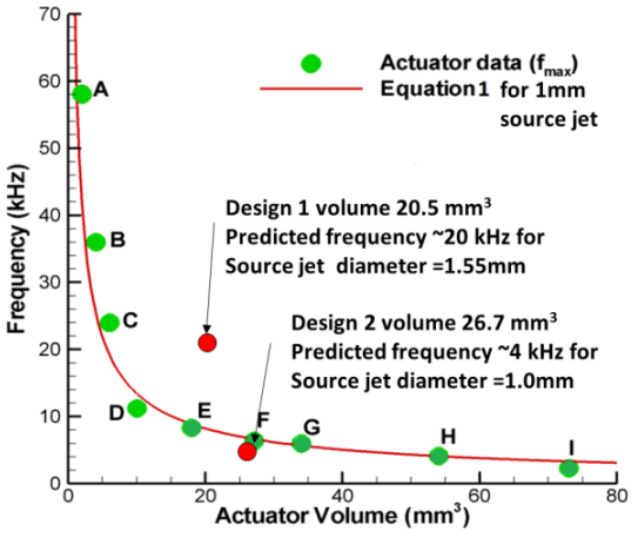

Fig.13 Frequency of REM-nozzle designs I and II plotted against the semi-empirical formula and previous data reported in reference [25]

For second nozzle, the design volume is 26.7 mm^3 and it uses a source jet nozzle of diameter 1 mm. The equation 1, discussed in section I, predicts a maximum resonance frequency of 4 kHz for this REM nozzle. The data shows that the maximum frequency of second nozzle is measured 3.7 kHz, fairly close to this prediction. In the next section, the flowfield of REM-nozzles captured using the lens based Microschlieren system is described.

C. Microschlieren images of REM –Nozzle flowfield

The REM-nozzle flowfield is captured using the specialized microschlieren system designed and assembled for the current study as shown earlier in Fig 3. This system uses a LED light source that produces white light with a pulse width less than 80 *ns*. Using this extremely short light pulses, we 'froze' and captured the fast-moving structures of this microscale flow. MATLAB™ code is used for the post processing and background subtraction of

the acquired images. Figure 14*a-c* shows three distinct phases of REM actuator flowfield of design I when no CO_2 is injected through the assembly. The images shown in fig. 14 correspond to the case when the actuator is pulsing at a frequency of 21 kHz.

It is evident that the pulsing of the micro jet creates compressible vortices that are moving at high speed and at this ultra-high frequency. Highly unsteady oscillating flow is noticed at the impinging side of the source jet. The initial pulsing phase of the actuator jet is shown in Fig. 14*a*. A compressible vortex begins to appear with a bow shock upstream of the flow. Fig 14*b* shows another phase of the evolution of this compressible vortex further downstream. As it evolves it entrains more fluid and diffuses downstream. It is evident that the evolving jet is supersonic with the presence of shock cells and oblique shock patterns in the flow.

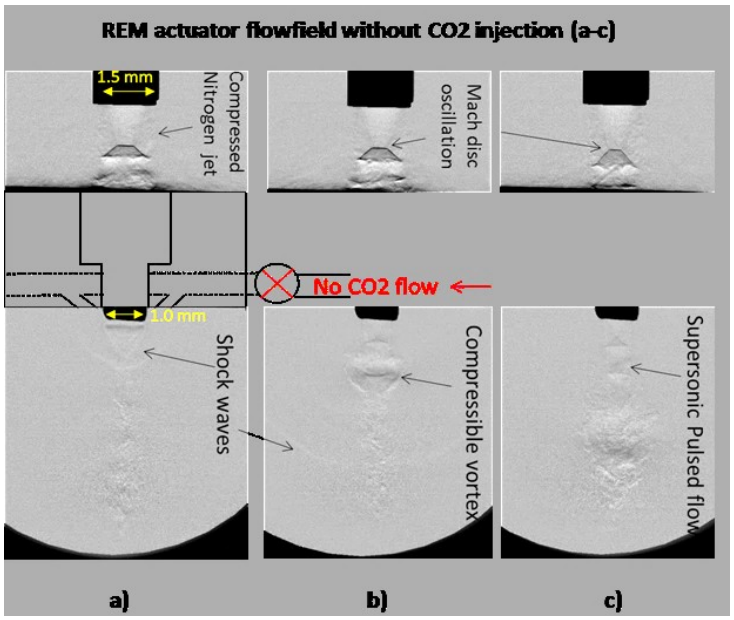

Fig.14 Three distinct phases of REM actuator flowfield of design I when no CO_2 is injected through the assembly.

Figure 15 shows representative images of the flowfield of CO2 jet injected through the four nozzles in the REM-nozzle assembly at 20 psi. There are no actuation jets operating in this case. The plume from four 400 micrometer diameter nozzles initially converges to the center and then spreads downstream with an included angle of nearly 60°. Merging of four jet plumes attributes turbulent features to this flowfield. Figure 16 *a-c* shows the instantaneous REM nozzle flowfield when CO_2 injected at 20 psi is mixed with the air jet pulsing at 21 kHz. These images show

that the pulsed air jet entrains the CO_2 jet and grows downstream with very high speed. It combines the features described in Figure 14 and 15, where actuator flow and injected fluid were visualized separately. Fig. 16*a* shows the beginning phase of pulsing in which a compressible vortex is appearing near the nozzle lip within the injected fluid. The phases shown in Fig.16*b&c* indicate its further diffusive movement. A careful observation of Fig. 15 and 16 indicates that the injected jet plume divergence has slightly reduced due the vortex generated entrainment.

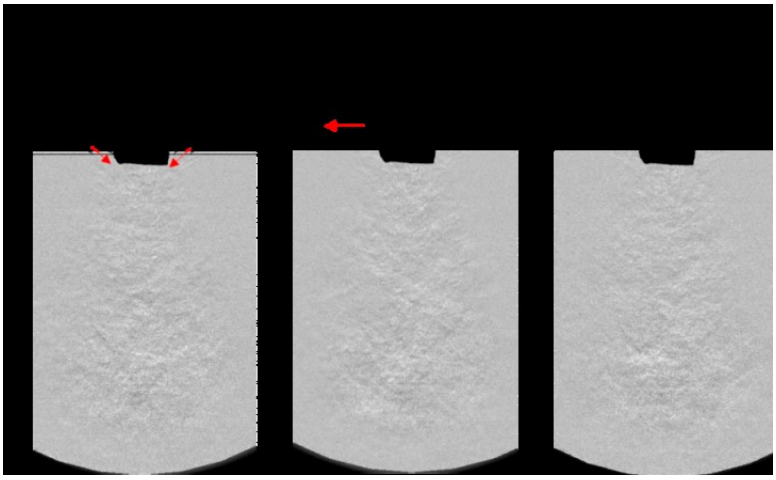

Fig.15 Flowfield of CO2 jet injected through the four nozzles in the REM-nozzle design I. No actuator jet is operational in this case.

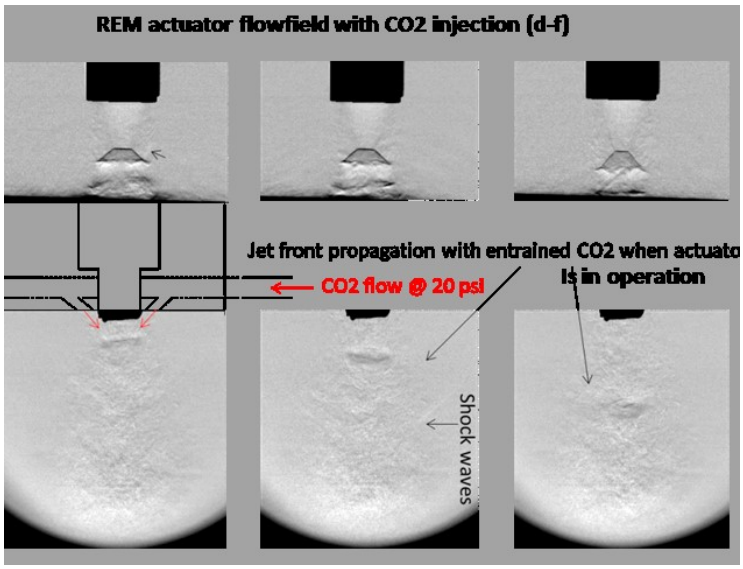

a) **b)** **c)**

Fig. 16 Microschlieren images of REM nozzle design 1, when CO_2 is injected while the actuator jet is oscillating at 21 kHz.

It evident that using design I, the injecting fluid can be entrained into the high frequency pulsing jet's vortices (that constitutes air, which is an oxidizer). This trapped fluid (fuel)-oxidizer mixer can be pushed downstream with high momentum. For applications as mentioned in fig. 1, such a fuel injection scheme maybe explored for better mixing and combustion efficiency. The design 1 essentially leverages a remarkable property of REM actuator technology to produce pulsed vortex at very high frequency and at very high speed. While entrainment properties of pulsed flow are exploited in the design I, design II uses REM actuator's capability to alter the natural instabilities of the shear layer of an injecting fluid. In this case pulsed actuators were injected to a fluid jet to induce rolling vortices in its shear layer. Although we limit our discussions on the design, fabrication details and flow characteristics of these two designs in this paper, studies are ongoing to understand their mixing characteristics and effectiveness quantitatively.

Temporal characteristics of REM actuator source jet oscillations

To understand the ultra-high frequency characteristics of the pulsed flow and the highly unsteady oscillatory nature of the Mach disc of the REM actuator source jet, the flowfield is captured at higher frame rates. Fig 17 shows six time resolved images of source jet with 16 micro second interval (64 kHz frame rate) captured at a lower resolution (1280x72 pixels). The corresponding resonance peak is measured as12.72 kHz as shown in Fig. 18*a*. The exposure time of the camera is set 1/250000 seconds to freeze the fast-moving shock structures at this scale. Since the actuator is pulsing at 12.72 kHz, 5-6 images were captured for the 1 complete cycle of the periodic oscillation of the source jet. To better understand the oscillatory nature of the source jet and its correlation to the nearfield microphone data, these images captured in each cycle are analyzed using *ImageJ* analysis software and MATLAB. The oscillations frequency, displacement and average velocity fluctuation of the Mach disc were estimated using this technique as discussed below.

Oscillation Frequency, displacement and average velocity of Mach disc

The Fig. 19 shows representative images of Mach disc oscillations of two cycles. The displacement of Mach disc is 380 micrometers for a period of 0.039 milliseconds. This will provide an average velocity of 9.74 m/sec for the shock motion. The period of oscillation is measured as 0.078 milli seconds and the corresponding frequency is calculated as 12.8 kHz for both sets of images. The nearfield pressure spectra measured by the microphone

captures this frequency as 12.72 kHz (fig. 18*a*), which is very close to this calculation. It is evident that these Mach disc oscillations, which are correlated to the filling and spilling phases of actuator, is responsible for the discrete tones in the nearfield. For more statistically accurate estimate of Mach disc oscillation frequency, a sample of two thousand and three (2003) images were analyzed using the *ImageJ* software as shown in Fig. 20.

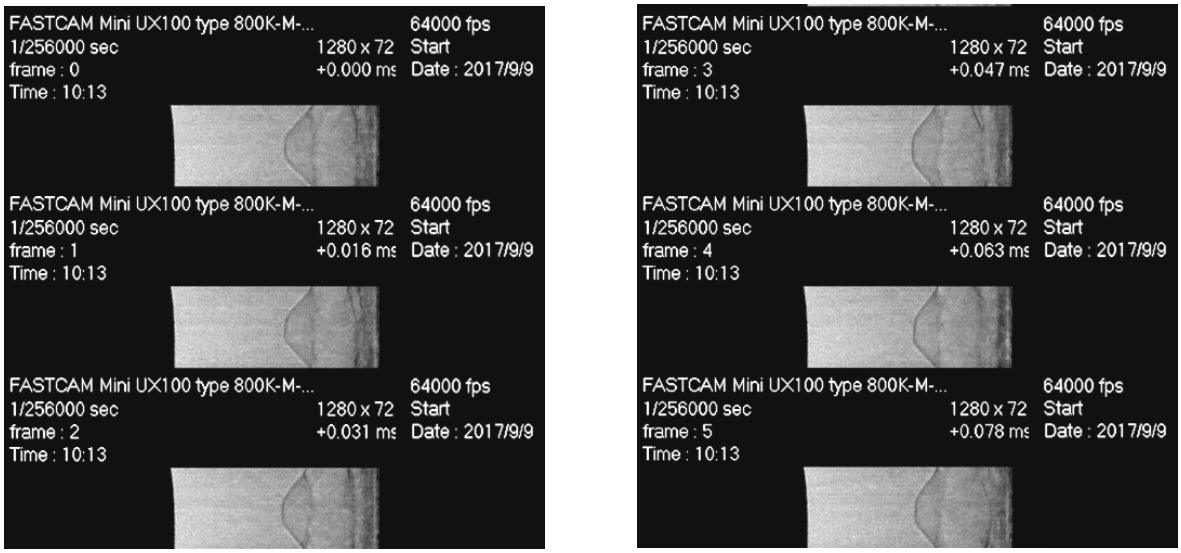

Fig. 17 Oscillatory source jet of actuator captured at 1250x72 pixel resolution and 64 kHz frame rate.

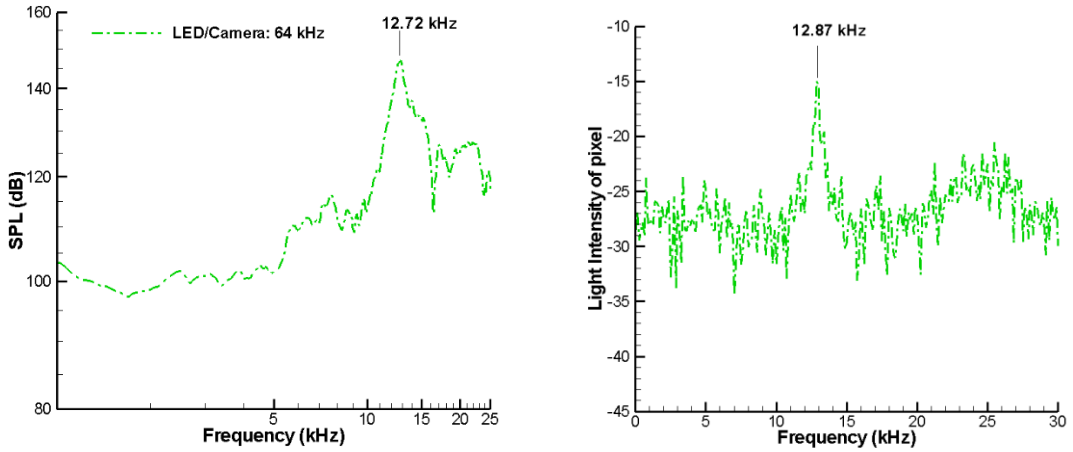

a) **b)**

Fig. 18 Frequency spectra of actuator source jet measured using a) the microphone b) Estimated using image analysis

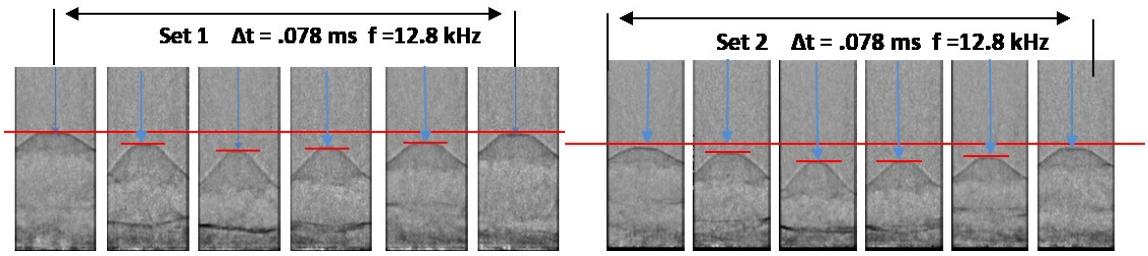

Fig. 19 Mach disc oscillation of source jet images (two sets) captured at 64 kHz frame rate

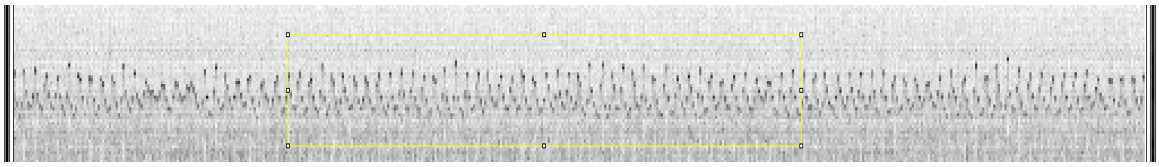

Fig. 20 Intensity of 1D array of pixels that contains Mach disc location, sequentially arranged for 2003 images

Fig. 20 shows image intensity of a 1D array of pixels that contains Mach disc location sequentially arranged for 2003 temporal images and analyzed using *ImageJ* software. This representation captured the transient oscillation of Mach disc more systematically. This processed image matrix is then analyzed using MATLAB^{TM} to find the maximum intensity value and its frequency using an fft analysis. This data shown in Fig. 18*b* indicates the frequency of oscillation as 12.87 kHz which is matching with the predictions from the sample sets and microphone data.

Temporal Characteristics of pulses actuation jet

The instantaneous global flowfield of the REM-nozzle, as shown earlier in Figure 16, indicates pulsed actuator flow evolution with entrained injected fluid. To quantify mixing of pulsed actuation jet and the mixing fluid, the velocity of the pulsed vortex is required. A typical jet front motion is shown in Figure 21*a*. To capture the temporal evolution of the fast-moving microscale jet front, and to find the velocity, image pairs were captured at a lower resolution of 1280x32 pixels at higher frame rate of 100 kHz with camera exposure of 3.9065 microseconds as indicated in Fig 21*b*.

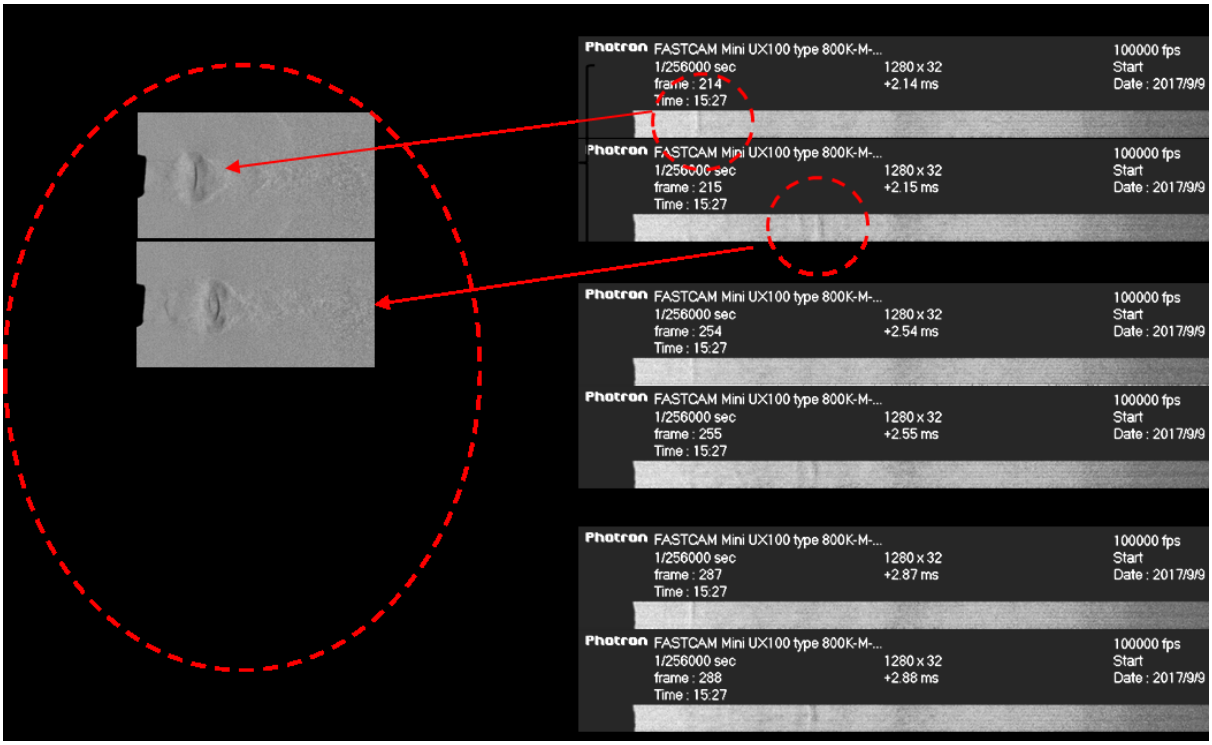

a) b)

Fig. 21 Image pairs used to calculate the speed of pulsed vortex generated by the REM-Nozzle.

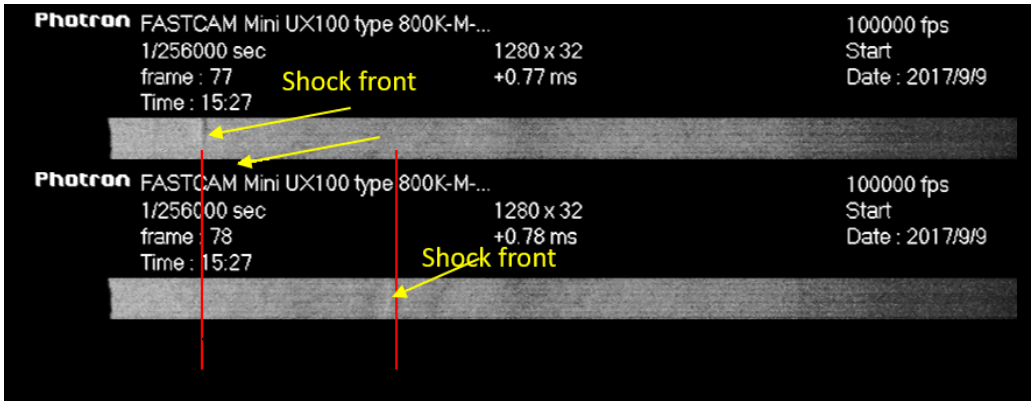

Fig. 22 Temporal evolution of Jet front captured by two consecutive images captured at 100 kHz frame rate

As explicitly indicated in Fig. 22, the compressible vortex wave front travels 2 mm in 10 microseconds. The average velocity is calculated as 200 m/sec in all the sample image pairs.

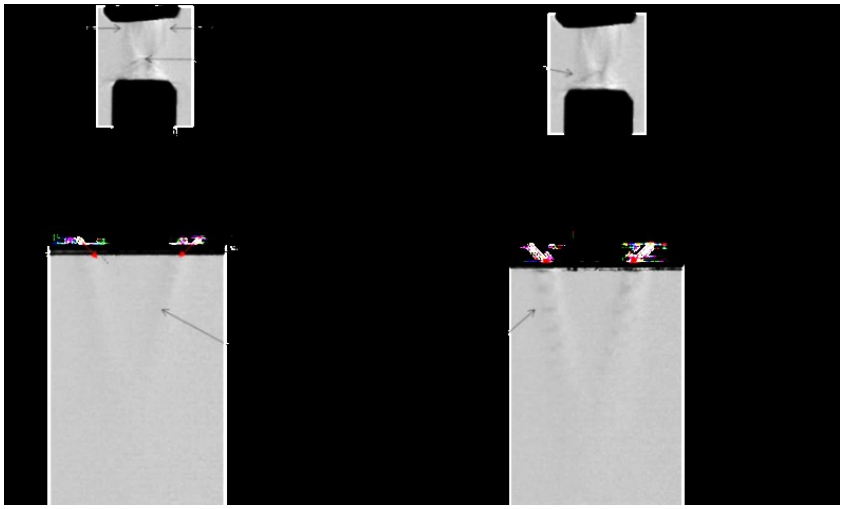

a) b)

Fig. 23 Microschlieren images of REM nozzle design 2 *a)* without CO2 injection when actuator is operating at 2.3 kHz and jet is subsonic *b)* when the pulsing jet is supersonic

Figure 23 shows flowfield of the REM-nozzle design II in which pulsed actuators are integrated symmetrically near the circumference of a 1mm nozzle through which steady CO2 is injected. Fig. 23*a&b* shows two distinct phases of pulsing, one subsonic and the other supersonic, of four 400 micrometer diameter jets when no mixing fluid is injected through the nozzle. In this case the actuator source jet is supplied from a nozzle of 1mm diameter. The pulsed microjets which are inclined at an angle of 30° to the vertical axis infuse streamwise vorticities in the shear layer of the injecting fluid in a frequency range of 2-4 kHz.

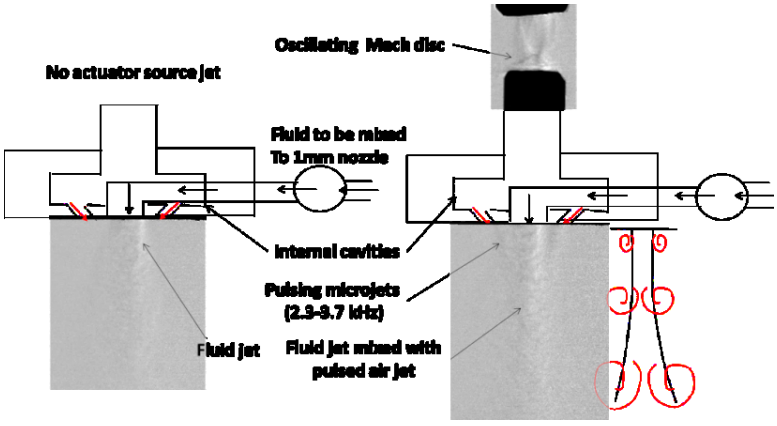

a) b)

Fig. 24 Microschlieren images of REM nozzle design II a) CO2 injection at 20 psi without actuator flow b) CO2 injection when actuator jets are pulsing at 2.3 kHz

Figure 24*a* shows instantaneous microschlieren images of the REM nozzle II when the mixing fluid CO_2 is injected through the 1.0 mm diameter nozzle. No actuator jet is used in this case. Fig. 24*b* shows REM nozzle flowfield when CO2 is injected while actuator jets are in pulsing mode with the operational parameters h/d=1.3 and NPR=4.5. To better understand the expected feature of pulsed actuator interaction on the shear layer of the injected fluid, an additional sketch is shown along with the microschlieren image. The pulsed microjets operating at 2.3 kHz are expected to generate rolling vortices in the same frequency range with enhanced entrainment properties.

In summary, the data from the nearfield microphone and the qualitative schlieren images of REM –nozzle design I and II demonstrate that these actuator-assisted nozzle designs have the capability to generate high frequency compressible vortices inside a high-speed injecting fluid. Such designs are expected to enhance entrainment at higher velocities, a characteristic that can be exploited for high-speed mixing applications.

V Conclusions

In this paper, we report the design, development, and detailed characterization of two high-frequency microactuator based nozzle assemblies (REM-nozzles) that can be used for high-speed flow mixing applications. In the first design, four micronozzles of 0.4 mm diameter are integrated close to the circumference of another nozzle through which a 1mm supersonic pulsed air jet flows out in the frequency range of 13-21 kHz. Steady CO_2 jets were injected through the micro nozzles in this study. In the second design, pulsed microjets in the frequency range of 2 - 4 kHz were integrated surrounding a 1mm nozzle through which a mixing fluid is injected. Using a specially designed microschlieren system that uses short LED light pulses the flowfield is captured and analyzed. In both designs the high frequency vortex generated due to the pulsing entrains the fluid injected into its evolution space and enhancing mixing while propagating downstream with very high speed. Such a nozzle configuration is expected to be useful for applications where high-speed mixing is required in a controlled manner. Quantitative characterization of mixing of both these nozzles is ongoing which will be reported in the future.

Acknowledgements

This work is supported by National Science Foundation through the grant 1504865. Authors also thank the

Master machinist Joe Wilson, Precision Prototype, Opelika, AL for fabricating the REM-Nozzle block assembly used in this study.

References

1. Seiner, J. M., Dash, S. M., and Kenzakowski, D. C., "Historical Survey on Enhanced Mixing in Scramjet Engines," Journal of Propulsion and Power, Vol. 17, No. 6, 2001, pp. 1273–1286.doi:10.2514/2.5876

2. Gutmark, E. J., Schadow, K. C., and Yu, K. H., "Mixing Enhancement in Supersonic Free Shear Flows," Annual Review of Fluid Mechanics, Vol. 27, Jan. 1995, pp. 375–417. doi:10.1146/annurev.fl.27.010195.002111

3. Bogdanoff, D. W., "Advanced Injection and Mixing Techniques for Scramjet Combustors," Journal of Propulsion and Power, Vol. 10, No. 2, 1994, pp. 183–190. doi:10.2514/3.23728

4. Lee, J., Cheng, K., and Eklund, D., "Challenges in Fuel Injection for High-Speed Propulsion Systems", AIAA Journal, Vol. 53, No. 6, pp. 1405-1423, 2015. doi.org/10.2514/1.J053280

5. Kraus, D. K., and Cutler, A. D., "Mixing of Swirling Jets in a Supersonic Duct Flow," Journal of Propulsion and Power, Vol. 12, No. 1, 1995, pp. 170–177. doi:10.2514/3.24007

6. Cutler, A. D., and Doerner, S. E., "Effects of Swirl and Skew Upon Supersonic Wall Jet in Crossflow," Journal of Propulsion and Power, Vol. 17, No. 6, 2001, pp. 1327–1332. doi:10.2514/2.5882

7. Pandey, K. M., Sivasakthivel, T., "Recent Advances in Scramjet Fuel Injection" International Journal of Chemical Engineering and Applications, Vol 1, No. 4, December 2010. ISSN: 2010-0221

8. Drozda, T.G., Baurle, R.A., Drummond, J.P., "Impact of Flight Enthalpy, Fuel Stimulant, and Chemical Reactions on the Mixing Characteristics of Several Injectors at Hypervelocity Flow Conditions", NASA Langley Research Center, May 2016. https://ntrs.nasa.gov/archive/nasa/casi.ntrs.nasa.gov/20160009131

9. Gruber, M. R., Nejad, A. S., Chen, T. H., and Dutton, J. C., "Transverse injection from circular and elliptic nozzles into a supersonic crossflow," Journal of Propulsion and Power, Vol. 16, No. 3, 2000, pp. 449-457. doi.org/10.2514/2.5609

10. VanLerberghe, W. M., Santiago, J. G., Dutton, J. C., and Lucht, R. P., "Mixing of a sonic transverse jet injected into a supersonic flow," AIAA Journal, Vol. 38, No. 3, 2000, pp. 470-479. doi.org/10.2514/2.984

11. Shigeru, A., ArifNur, H., Shingo, M., Kei, I., Yasuhiro, T., "Fundamental Study of Supersonic Combustion in Pure air flow with use of Shock Tunnel", Department of Aeronautics and Astronautics, Kyushu University, Japan , Acta Astronautica, Vol 57, Issues 2-8, 2005, pp.384 – 389. doi.org/10.1016/j.actaastro.2005.03.055

12. Menon, "Shock wave induced mixing enhancement in scramjet combustors," AIAA Paper 89–0104 1989 doi.org/10.2514/6.1989-104

13. Ben Yakar, Cavity Flame-Holders for Ignition and Flame Stabilization in Scramjets: An Overview, JPP J, Vol. 17, No. 4, 2001. doi.org/10.2514/2.5818

14. Ben-Yakar, B., Mungal, M. G., and Hanson, R. K., "Time evolution and mixing characteristics of hydrogen and ethylene supersonic crossflow," Physics of Fluids, Vol. 18, No. 2, 2006, pp. 026101 16. doi.org/10.1063/1.2139684

15. Hsu, K., Carter, C.D., Gruber, M. R., Tam, C., "Mixing Study of Strut Injectors in Supersonic Flows" AIAA Joint Propulsion Conference, August 2009. doi.org/10.2514/6.2009-5226

16. Hongbin G., Zhi, L., Fei, L., Lihong, C., Shenglong, G., Xinyu, C., "Characteristics of Supersonic Combustion with Hartmann-Sprenger Tube Aided Fuel Injection", AIAA Conference, 2011. doi.org/10.2514/6.2011-2326

17. Kouchi, T., Sasaya, K., Watanabe, J., Sibayama, H., Masuya, G., "Penetration Characteristics of Pulsed Injection into Supersonic Cross flow", AIAA Joint Propulsion Conference. 2010. doi.org/10.2514/6.2010-6645

18. Cutler, A.D., Harding, G.C., Diskin, G.S., "High Frequency Pulsed Injection into a Supersonic Duct Flow", AIAA Journal, 2013, Vol.51: 809-818, 10.2514/1.J051620.

19. Joussot, R., Coumar, S., Lago, V., "Plasmas for High Speed Flow Control", Aerospace Lab Journal, Issue 10, 2015. 10.12762/2015.AL10-04

20. Utkin, Y.G., Keshav, S., Kim, J., Kastner, J., Adamovich, I., Samimy, M., "Development and Use of Localized Arc Filament Plasma Actuators for High Speed Flow Control", Journal of Applied Physics, Vol 40. 2007. doi.org/10.1088/0022-3727/40/3/S06

21. Johari, H., "Scaling of Fully Pulsed Jets in Crossflow," AIAA Journal, Vol. 44, No. 11, 2006, pp. 2719–2725. doi:10.2514/1.18929.

22. H. Johari, M. Pacheco-Tougas, and J. C. Hermanson, "Penetration and mixing of fully modulated turbulent jets in crossflow," AIAA J. 37, 842 1999. doi.org/10.2514/2.7532

23. F. E. Marble, E. E. Zukoski, J. W. Jacobs, G. J. Hendrick, and I. A. Waitz, "Shock enhancement of and control of hypersonic mixing and combustion," AIAA Paper 90–1981 1990 doi.org/10.2514/6.1990-1981

24. Solomon, J. T., Kumar, R., and Alvi, F.S., "High-Bandwidth Pulsed Microactuators for High-Speed Flow Control," AIAA Journal, Vol. 48, No. 10, pp. 2386-2396, 2010. doi.org/10.2514/1.J050405

25. Solomon, J. T., Foster, C., Alvi F.S., "Design and characterization of High-Bandwidth, Resonance Enhanced, Pulsed Microactuators: A parametric Study", AIAA Journal, Volume 51, No. 2, pp 386-396, 2013. doi.org/10.2514/1.J051806

26. Solomon, T, J., "High-bandwidth Unsteady Actuators for Active Control of High-Speed Flows," PhD Dissertation, Florida State University, 2010. http://purl.flvc.org/fsu/fd/FSU_migr_etd-1642

27. Topolski, N., Arora, N., Ali, M.Y., Solomon, J.T., Alvi, F.S., "Experiments on Resonance Enhanced Microactuators in Supersonic Crossflow", AIAA-2813, 2012 10.2514/6.2012-2813

28. Kreth, P., Solomon, J.T., Alvi, F.S., “Resonance-Enhanced High Frequency Micro-actuators with Active Structures”, AIAA-2939, 2011. 10.2514/6.2011-2939

29. Upadhyay, P., Gustavsson, J., Alvi, F.S., “Development and Characterization of Ultra-High Frequency Resonance Enhanced Microactuators”, AIAA-2476, 2013. 10.2514/6.2013-2476

30. Foster, C., Solomon, J.T., Alvi, F.S., “Visual Study of Resonance dominated Microjet flows using laser based micro-Schlieren”, AIAA-2011-766, 2011. doi.org/10.2514/6.2011-766

31. Uzun, A., Solomon, J.T., Foster, C.H., Oates, W.S., Hussaini, M.Y., Alvi, F.S., "Simulations of Pulsed Microactuators of High -Speed Flow Control", AIAA *Journal* Volume 51, No. 12, pp 2894-2918, **2013.** doi.org/10.2514/1.J052525

32. Strickland, G., Solomon, J.T., Gustavson, G., Alvi, F.S., “Implementing Resonance Enhanced Microactuators for the control supersonic microjets”, AIAA-0065, 2012. 10.2514/6.2012-65

33. Solomon, J.T., Hong, S., Wiley, A., Kumar, R., Annaswamy, A.M., Alvi, F.S., “Control of Supersonic Resonant flows Using High bandwidth Micro- Actuators”, AIAA -3247, 2009. doi:10.2514/6.2009-3247

34. Ali, M.Y., Solomon, J.T., Gustavsson, J.P.R., Alvi, F.S., “Control of Supersonic Cavity Flows Using High Bandwidth Micro actuators”, AIAA-197194-564, 2010. doi:10.2514/6.2010-1198

35. Ali, M., Arora, N., Topolski, N., Alvi, F.S., Solomon, J.T., "Properties of Resonance Enhanced Microactuators in Supersonic Crossflow", AIAA *Journal,* Vol. 55, No. 3 (2017), pp. 1075-1081 http://dx.doi.org/10.2514/1.J055082

36. Upadhyay, P, Gustavsson, J.P.R., Alvi, F.S., “Development and Characterization of High-frequency Resonance Enhanced Microactuators for Control of High-Speed Jets”, Exp Fluids (2016) 57:88 DOI 10.1007/s00348-016-2164-2

37. Dziuba, M, Fay, J, and Rossmann. T.,"Detailed Study of Mixing Enhancement by Jet Modulation and Oblique Injection", AIAA-0117-2007 https://doi.org/10.2514/6.2007-117